Supporting Information

Origin of anisotropic thermal transport in $CsPbBr_3$

Wilarachchige D. C. B. Gunatilleke,[a] Oluwagbemiga P. Ojo[a], and George S. Nolas*[a]

[a]Department of Physics, University of South Florida, Tampa, FL 33620, USA

$CsPbBr_3$ Crystal Growth

A single crystal of $CsPbBr_3$ was grown from the melt using optimized Bridgman growth (Figure S1). The microcrystalline powder for the melt was obtained from the direct reaction of CsBr (Sigma Aldrich, 99.999%) and $PbBr_2$ (Sigma Aldrich, 99.999%) in 1:1 stoichiometric ratio at 923 K for 24 h. The as-synthesized microcrystalline product was subjected to multiple zone refinement processes for optimum purity. A pointed quartz crucible with an inner diameter of 10 mm was loaded with the zone refined $CsPbBr_3$ and sealed under vacuum in a quartz tube with a large empty space above the crucible. It was observed that this volume above the crucible was crucial in obtaining one single crystal during Bridgman growth. Grain boundaries resulted during cooling of the melt in the absence of this empty space above the melt. The melt temperature was maintained between 863 K and 873 K for 6 hr to ensure homogeneity of the melt prior to translational motion for crystal growth. The translational motion of the melt was controlled at a rate of 0.7 mm/hr until the melt temperature dropped below 798 K, at which point the melt was slowly cooled down at a rate of 5 K/hr until the temperature of the melt dropped below 773 K to induce crystallization before cooling down to room temperature at a rate of 10 K/hr. A disc was cut from the large single crystal to investigate the thermal transport. A parallelepiped of 2.0 x 2.5 x 3.0 mm^3 was then cut from the disc for temperature dependent thermal conductivity, κ, measurements.

Structural Characterization

The crystal structure was analysed by Rietveld structure refinement of the X-ray diffraction (XRD) data collected after grinding a portion of the crystal. Powder XRD data were collected with a Rigaku SmartLab diffractometer in Bragg–Brentano geometry with Cu Kα radiation. Rietveld refinement was performed using GSAS II software [1] to investigate the isotropic and anisotropic displacement parameters for $CsPbBr_3$, as described in the article. The initial parameters for structure refinement were based on structural data previously reported[2]. The Rietveld structure refinement results for the phase-pure microcrystalline powder of $CsPbBr_3$ used for Bridgman growth are given in Figure S2 and Tables S1. The atomic displacement parameters are given in Tables S2 and S3. These results are in excellent agreement with the reported structural parameters for $CsPbBr_3$ [2]. Extensive XRD investigations were undertaken for crystal orientation, and the orientation of the lattice planes of the crystal along the directions of the thermal conductivity measurements were determined by XRD as shown in Figure S3.

Thermal Properties Measurements

The DynaCool Physical Property Measurement System (PPMS) from Quantum Design was used for temperature dependent thermal transport measurements. The Thermal Transport Option (TTO) module and Heat Capacity (HC) module were used to measure κ and C_p respectively. Figure S4 shows the crystal specimen mounted for thermal conductivity measurements. The κ measurements were performed from 300 K to 2 K in a two-probe configuration under continuous sweep mode at a rate of 0.3 K/min. The crystal specimens were attached to the TTO module using Au coated manganin leads using Ag epoxy (H20E). Our PPMS κ data are calibrated based on measurements from a custom-built instrument employing standards [3]. Thermal N-grease was used to couple the crystal specimen with the mounting stage of the HC module. The measurements were performed from 300 K to 2 K with a 2% temperature rise. The two-tau model of the Quantum Design heat capacity software was used for the measurements. Appropriate addendum measurements preceded the heat capacity measurements. Maximum experimental uncertainties of ± 6% and ± 5% were calculated for κ and C_p data, respectively.

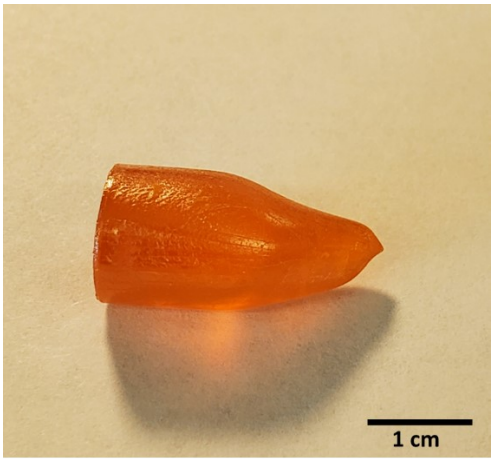

Figure S1. A single crystal of $CsPbBr_3$ obtained from Bridgman growth.

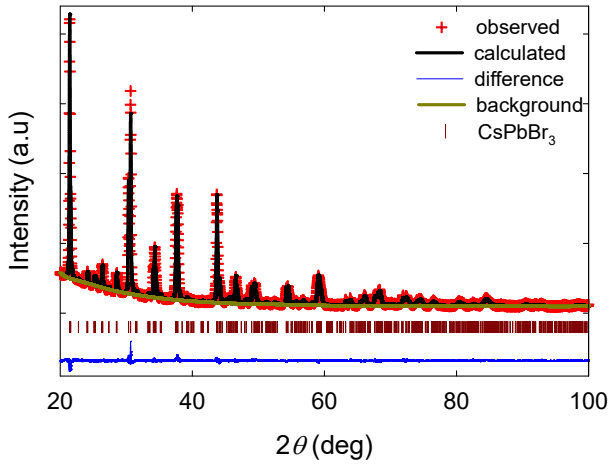

Figure S2. Powder X-ray diffraction pattern of $CsPbBr_3$, together with the calculated profile, difference profile and Bragg positions from Rietveld refinement.

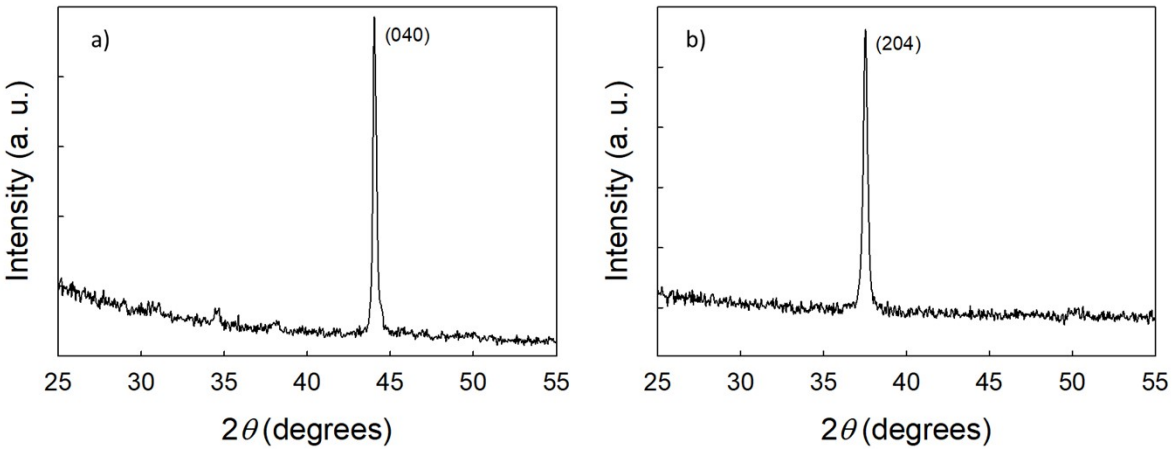

Figure S3. XRD spectra indicating the orientation of (a) the *a*-*c* plane, i.e. the (0*k*0) planes and (b) the (204) plane on the specific surfaces of the crystal specimen employed for thermal conductivity measurements that are represented in Figure 2 of the article.

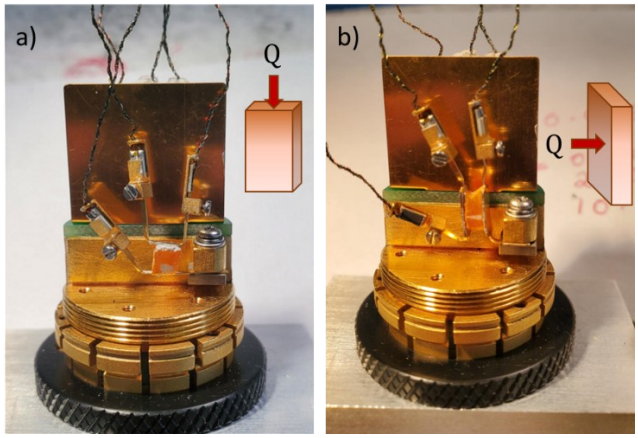

Figure S4. Crystal specimen mounted on the TTO module of the PPMS for the measurement of thermal conductivity a) parallel and b) perpendicular to the (204) plane. The direction of the heat flow (Q) across the specimen is also indicated.

Table S1. Summary of Rietveld refinement results.

crystal system	orthorhombic
space group	*Pbnm* (#62)
a (Å)	8.2031(15)
b (Å)	8.2517(16)
c (Å)	11.7510(22)
V (Å^3)	795.4(5)
Z	4
mol. w. (g/mol)	579.82
d_{calc} (g/cm^3)	4.8417
Radiation	Graphite monochromated Cu Kα (1.5406 Å)
2θ range (^{o})	20 - 100
*wR*p, *R*p	0.03792, 0.02929
GOF	1.308

Table S2. Atomic coordinates, Wyckoff position, fractional occupancy, and isotropic atomic displacement parameters.

atom	site	*x*	*y*	*z*	Occ	U_{iso}(Å^2)
Cs	4*c*	0.9939(7)	0.9714(5)	0.25	1	0.104
Pb	4*b*	0.5	0	0	1	0.048
Br1	4*c*	0.0465(8)	0.5021(11)	0.25	1	0.111
Br2	8*d*	0.7918(4)	0.2097(5)	0.0221(4)	1	0.088

Table S3. Anisotropic atomic displacement parameters.

atom	U_{11}(Å^2)	U_{22}(Å^2)	U_{33}(Å^2)	U_{12}(Å^2)	U_{13}(Å^2)	U_{23}(Å^2)
Cs	0.1206(28)	0.106(3)	0.0842(21)	0.0351(31)	0	0
Pb	0.0583(15)	0.0385(14)	0.0466(13)	0.0024(27)	-0.0016(19)	0.0022(18)
Br1	0.141(7)	0.163(7)	0.0282(25)	0.022(8)	0	0
Br2	0.0727(29)	0.0687(30)	0.122(4)	-0.0354(21)	-0.014(4)	0.023(4)

References

[1] B. H. Toby, R. B. Von Dreele, *J Appl Cryst* **2013**, *46*, 544–549.

[2] C. A. López, C. Abia, M. C. Alvarez-Galván, B.-K. Hong, M. V. Martínez-Huerta, F. Serrano-Sánchez, F. Carrascoso, A. Castellanos-Gómez, M. T. Fernández-Díaz, J. A. Alonso, *ACS Omega* **2020**, *5*, 5931–5938.

[3] J. Martin, G. S. Nolas, *Review of Scientific Instruments* **2016**, *87*, 015105.